Available online at www.sciencedirect.com
SCIENCE DIRECT®
Biomaterials 26 (2005) 23–36
Biomaterials
www.elsevier.com/locate/biomaterials

Biological performance of uncoated and octacalcium phosphate-coated Ti6Al4V

Pamela Habibovic[a,*], Jiaping Li[a], Chantal M. van der Valk[b], Gert Meijer[c], Pierre Layrolle[d], Clemens A. van Blitterswijk[a], Klaas de Groot[a]

[a] *Institute of Biomedical Technology, Department Bilthoven, Twente University, Professor Bronkhorstlaan 10-D, Bilthoven 3720 MB, Netherlands*
[b] *IsoTis SA, Professor Bronkhorstlaan 10-D, Bilthoven 3720 MB, Netherlands*
[c] *University Medical Center Utrecht, PO Box 85500, Utrecht 3508 GA, Netherlands*
[d] *INSERM EM9903, Materials of Biological Interest, Faculty of Dental Surgery, Place Alexis Ricordeau, Nantes 44042, France*

Received 29 September 2003; accepted 3 February 2004

Abstract

The in vivo behavior of a porous Ti6Al4V material that was produced by a positive replica technique, with and without an octacalcium phosphate (OCP) coating, has been studied both in the back muscle and femur of goats. Macro- and microporous biphasic calcium phosphate (BCP) ceramic, known to be both osteoconductive and able to induce ectopic bone formation, was used for comparison purpose.

The three groups of materials (Ti6Al4V, OCP Ti6Al4V and BCP) were implanted transcortically and intramuscularly for 6 and 12 weeks in 10 adult Dutch milk goats in order to study their osteointegration and osteoinductive potential.

In femoral defects, both OCP Ti6Al4V and BCP were performing better than the uncoated Ti6Al4V, at both time points. BCP showed a higher bone amount than OCP Ti6Al4V after 6 weeks of implantation, while after 12 weeks, this difference was no longer significant.

Ectopic bone formation was found in both OCP Ti6Al4V and BCP implants after 6 and 12 weeks. The quantity of ectopically formed bone was limited as was the amount of animals in which the bone was observed. Ectopic bone formation was not found in uncoated titanium alloy implants, suggesting that the presence of calcium phosphate (CaP) is important for bone induction.

This study showed that CaPs in the form of coating on metal implants or in the form of bulk ceramic have a significantly positive effect on the bone healing process.

Keywords: Porous Ti6Al4V; Biomimetic coatings; Octacalcium phosphate (OCP); Biphasic calcium phosphate (BCP); Osteointegration; Osteoinduction

1. Introduction

Calcium phosphate (CaP) containing biomaterials, in particular hydroxyapatite (HA), beta tricalcium phosphate (β-TCP), and the mixtures of two, are known for having a good biological performance [1–5], but they often lack satisfactory mechanical properties.

Metals, on the other hand, possess great mechanical properties, making them suitable for load-bearing applications [6]. However, high stiffness of the metals often leads to stress-shielding from residual bone, which may result in detrimental resorptive bone remodeling [7], and consequently to a poor fixation of the implant. Recent developments in metallic implant designs therefore focus on adapting the mechanical properties of metals to those of biological systems. Certain metals, such as stainless steel, titanium and its alloys, are already widely used in orthopedics and dentistry because of their good biocompatibility [8,9], but their abilities to bond to bone and to guide bone growth are distinctly smaller as compared to the above-mentioned ceramics.

Recent designs of orthopedic implants therefore often include combinations of metallic and CaP materials. One example is the application of CaP coating on metal implants that combines the mechanical strength of the metal with the ceramics favorable biological properties. In addition to the interfacial bonding to bone

*Corresponding author. Tel.: +31-302295298; fax: +31-302280255.
E-mail address: p.habibovic@tnw.utwente.nl (P. Habibovic).

0142-9612/$ - see front matter © 2004 Elsevier Ltd. All rights reserved.
doi:10.1016/j.biomaterials.2004.02.026

introduced by CaP coatings on dense metal implants, applying a porous structure can even further advance bony integration, whereby mechanical interlocking may also enhance the integration process.

Porous titanium and its alloys have been used in dental and orthopedic applications since the end of the 1960s [10–12]. Many available methods of producing porous titanium and titanium alloy scaffolds include sintering together of the particles [13,14] or plasma spraying (PS) of the powder on a dense substrate followed by the cutting of the porous layer [15]. The shortcoming of these production methods is that they often result in a low porosity (<50%), low average pore size (<300 μm) and poorly interconnected pores. All these factors might have a negative effect on the biological performance of these materials. Another method includes compacting single titanium fiber into a die to certain porosity, followed by vacuum sintering, resulting in the formation of a so-called titanium fiber mesh [15]. Besides excellent biocompatibility [16], sintered titanium fiber meshes have been shown to act as a good carrier for growth factors [17,18] and as tissue engineering scaffold [19,20]. However, in the absence of the growth factors and/or osteogenic cells, their osteoconductive performance is limited. In addition to titanium and its alloys, promising reports on the use of porous metals based on tantalum (Ta) for orthopedic applications have been given [21–23].

Our group has recently developed a porous Ti alloy material by using a positive replica technique. This technique allows us to produce a controllable high porosity structure, with open and interconnected pores [24].

As mentioned earlier, apart from the mechanical interlocking provided by implant porosity, applying a bioactive coating on the metal surface could further enhance its biological performance. The conventional technique to provide metallic implants with a CaP coating is PS. Earlier investigations have shown that these coatings can successfully enhance clinical success to a <2% failure rate after 10 years [25]. Despite this clinical performance, the PS method is limited by some intrinsic drawbacks. For instance, the coating is being produced at very high temperatures, limiting this method to stable CaP phases. Furthermore, by using this line-of-sight method, it is impossible to coat geometrically complex and porous implants.

One of the alternative methods uses the so-called biomimetic route, in which the bone mineralization process is mimicked by immersing implants in simulated body fluids (SBFs) [26]. As a result of the paraphysiological conditions of this technique, various CaP phases such as octacalcium phosphate (OCP) [27] or bone-mineral like carbonated apatite (CA) [28] can be deposited. A previous study in femoral condyle of goats by Barrère et al. [29] showed a direct contact between the newly formed bone and the OCP-coated porous Ta surface. Between the newly formed bone and uncoated Ta however, a layer of fibrous tissue was often observed. Intramuscular implantation of the OCP-coated porous Ta implants also showed the ability of such an implant to induce bone in non-osseous site, i.e. osteoinductive behavior [29–31].

The objective of this goat study was to investigate the biological performance of a porous titanium alloy (Ti6Al4V) material, produced by a positive replica method, with and without biomimetic OCP coating, in terms of osteointegration and osteoinduction.

2. Materials and methods

2.1. Implants

Porous titanium alloy (Ti6Al4V) implants were produced by a positive replica method as described earlier [24]. In short, 70 wt% of titanium alloy powder (Northwest Non-Ferrous Institute of China) consisting of spherical particles with a diameter lower than 44 μm (325 mesh) was mixed with H_2O (20 wt%). Polyethylene glycol (PEG) and methylcellulose were used as binders (8 wt%). Dolapix and ammonia solution (2 wt%) were added to improve the rheological property of slurry. Porous titanium alloy bodies were made by impregnation of polymeric (PU) sponges (35–45 pores/in) (Coligen Europe B.V., Breda, The Netherlands). When the slurry reached the designed viscosity range (3000–5000 cp), polyurethane (PU) foams were dipped into the slurry and then extracted to dry. The dipping–drying process was repeated until the struts of the PU foam were coated with titanium alloy slurry. The superfluous slurry was removed by using a roller under pressure, to get an evenly distributed coating on the foam. After final drying, the samples were heated in argon to 500°C to burn out the foam. This process resulted in a small change of color of the metal, which suggests the formation of a thicker titanium oxide (TiO_2) layer. Finally, the metal bodies were sintered in a vacuum furnace (10–5 mbar) at 1250°C with holding time of 2 h. The energy dispersive X-ray (EDX) analysis (result not presented) showed a higher oxygen peak in comparison to the green body, confirming the formation of a thicker TiO_2 layer. Cylinders ($\varnothing 5 \times 10\,mm^2$) were machined by using a wire electric discharge machine, with demineralized water as medium. The ultrastructure of porous titanium alloy was characterized by using an environmental scanning electron microscope (ESEM; XL30, ESEM-FEG, Philips, The Netherlands) in the secondary electron mode. The porosity of the material was determined by both volume/weight method ($n = 3$) and by image analysis technique on the histological slides (10 cross-sections for 6-week implantation and 10 cross-sections for 12-week implantation). In the volume/

weight method the following calculation is made: 100%−[(weight of the porous implant/the weight a dense implant with the same size)∗100%]. For the second method, high resolution (300 dpi), low magnification (10 ×) digital micrographs were made of blinded sections. Using Adobe Photoshop 7.0, bone and material were pseudocolored, red and green, respectively. Image analysis was carried out with a PC-based system equipped with KS400 version 3.0 software (Carl Zeiss Vision, Oberkochen, Germany). Prior to measurement the system was geometrically calibrated with an image of a block of known dimensions. A program was developed in KS400 to quantitate the pore size for each pore and the material porosity. The porosity was determined as (total implant area-scaffold area)/total implant area∗100%. Pore interconnectivity was visually analyzed on the material cross-sections by using an ESEM. The compression strength of the material was 10.3 ± 3.1 MPa, as measured and reported earlier [24].

Porous biphasic calcium phosphate (BCP) implants were prepared by using the so-called H_2O_2 method as published earlier [32]. For the preparation of the ceramic, in-house made BCP powder was used. Porous green bodies were produced by mixing this powder with 2% H_2O_2 solution (1.0 g powder/1.2 ± 0.05 ml solution) and naphthalene (Fluka Chemie, The Netherlands) particles (710–1400 μm; 100 g powder/30 g particles) at 60°C. The naphthalene was then evaporated at 80°C and the green porous bodies were dried. Finally, the bodies were sintered at 1200°C for 8 h. These bodies were machined into cylinders ($\varnothing 5 \times 10\,mm^2$) using a lathe. The structure of porous BCP was characterized by using an ESEM. Porosity, pore size and pore interconnectivity were analyzed by the same techniques as described for the Ti alloy implants. Material composition and its crystal structure were determined by using Fourier transform infra red spectroscopy (FTIR; Spectrum100, Perkin-Elmer Analytical Instruments, Norwalk, CT) and X-ray diffraction (XRD; Miniflex, Rigaku, Japan). HA/β-TCP weight ratio in the BCP was calculated by comparing the BCP XRD pattern to the calibration patterns prepared from the powders with the known HA/β-TCP weight ratios. The specific surface area of the material was measured by using the Brunauer, Emett and Teller method (BET, cfDIN66131) (Institut des materiaux de Nantes L.C.S., Nantes, France). The compression strength of the used BCP was 3.4 ± 0.8 MPa (unpublished results).

2.2. Coating process

Prior to the coating process, porous Ti alloy cylinders were ultrasonically cleaned in acetone, ethanol and water. Next, they were soaked in SBF for 24 h at 37°C to seed the metal surface with calcium phosphate nuclei. The used SBF solution was five times more concentrated than Kokubo's SBF solution [26] (Table 1) in order to speed up the coating process. The supersaturation of the SBF solution was achieved by addition of slightly acidic CO_2 gas. The starting pH of the solution was 5.8. At the end of the process, the pH reached a value of 8.3.

Table 1
Inorganic composition (mM) of Kokubo's SBF, supersaturated SBFx5 and SCS

	Ion concentration (mM)							
	Na^+	K^+	Ca^{2+}	Mg^{2+}	Cl^-	HPO_4^{2-}	HCO_3^-	SO_4^{2-}
SBF	142.0	5.0	2.5	1.5	148.8	1.0	4.2	0.5
SBFx5	714.8	—	12.5	7.5	723.8	5.0	21.0	—
SCS	140.4	—	3.1	—	142.9	1.86	—	—

In order to produce crystalline OCP coatings, the implants were then immersed at 37°C in simulated calcifying solution (SCS) (Table 1) for 48 h with one replenishment. SCS was buffered at pH 7.4 by using the TRIS/HCl. The biomimetic methods of producing the two CaP layers have previously been described in detail [27,28]. The coating composition and crystallinity were investigated by using FTIR and XRD. Coating thickness was measured on 2D implant cross-sections by the automatic ESEM ruler. The specific surface area of the coating was determined by using the BET method.

2.3. Animals

This study was approved by the Dutch Animal Care and Use Committee. Ten adult Dutch milk goats were used in total and housed at Central Animal Laboratory Institute (GDL), Utrecht, The Netherlands, at least 4 weeks prior to surgery.

Before the surgical procedure, a dose of 0.1 ml in 5 ml of physiologic saline solution (± 1 ml/25 kg body weight) of Domosedan (Pfizer Animal Health BV, Capelle a/d Ijssel, The Netherlands) was administered by intravenous injection. The surgical procedure itself was performed under general inhalation anesthesia of the animals. Thiopental (Nesdonal, ± 400 mg/70 kg of body weight, on indication, Rhone Merieux, Amstelveen, The Netherlands) was injected intravenously, and anesthesia was maintained with a gas mixture of nitrous oxide, oxygen and Halothane (ICI-Farma, Rotterdam, The Netherlands).

Besides the implantations described in this study, the animals were used for a different study, to be published separately. Based on the previous in vivo studies by our group, we hypothesize that different groups of implants could not influence each other's behavior, as they were implanted either at a different implantation site or at a sufficient distance from each other.

2.4. Implantation in bone

The implants were inserted in the left diaphyseal femur of the goats, which was exposed by a lateral skin incision and blunt dissection. The holes were drilled in the lateral cortex using a pneumatically powered orthopedic drill (drilling speed 150 rpm), under permanent cooling with saline. Each defect was created according to a four-step procedure, to a final diameter of 5.0 mm. The implants (uncoated Ti6Al4V, OCP Ti6Al4V and BCP) were allocated according to randomized scheme. Using gentle tapping, the implants were press-fit inserted in their designated positions. The incision was routinely closed with sutures. After 6 weeks, the same procedure was repeated in the right diaphyseal femur of all goats. Table 2 gives an overview of the implanted materials.

2.5. Intramuscular implantation

After shaving the lumbar area and disinfection with iodine, the left muscle fascia was exposed and cut. Using blunt dissection, intramuscular pockets were created, and filled with the above-mentioned implants. Subsequently, the fascia was closed with a non-resorbable suture to facilitate implant localization at explantation. The skin was closed in two layers. After 6 weeks, the same procedure was repeated in the right back muscle. Table 2 shows the amounts of implanted materials.

Immediately after the surgery, pain relief was given by buprenofine (Temgesic; Schering-Plough, Kenilworth, NJ).

Twelve weeks after the first implantation (i.e. implantation times 6 and 12 weeks), each animal was sacrificed by an overdose of pentobarbital (Euthesaat, Organon, Oss, The Netherlands) and potassium chloride.

2.6. Retrieval of the implants, histology and histomorphometry

The implants from the retrieved femora were isolated "en block" using a diamond saw, and fixed at 4°C in Karnovsky's fixative (4% paraformaldehyde, 5% glutaraldehyde). Intramuscular implants with surrounding tissue were explanted by sharp dissection and fixed in Karnovsky's fixative as well. All implants were dehydrated in a graded ethanol series (70–100%) and transferred into a methylmethacrylate (MMA) solution that polymerized at 37°C within 1 week. Longitudinal sections (10–15 μm) were made by using the modified interlocked diamond saw (Leica Microtome, Nussloch, Germany). Sections were stained with 1% methylene blue and 0.3% basic fuchsin after etching with HCl/ethanol mixture. The midsections of the implants retrieved from femora were used for histomorphometry. In case of intramuscular implants, only qualitative analysis using a light microscope (E600 Nikon, Japan) was performed.

For histomorphometry of femora implants, high resolution (300 dpi), low magnification (10×) digital micrographs were made of blinded sections. Using Adobe Photoshop 7.0, bone and material were pseudo-colored, red and green, respectively. Image analysis was carried out with a PC-based system equipped with KS400 version 3.0 software (Carl Zeiss Vision, Oberkochen, Germany). Prior to measurement the system was geometrically calibrated with an image of a block of known dimensions. A program was developed in KS400 to quantitate different parameters concerning bone formation:

1. *%b.cont. in cortex*: percentage of available scaffold outline (which is the surface of the scaffold) in contact to bone: [% contact = (bone-scaffold contact length/scaffold outline length)∗100%] within the cortical area (area C in Fig. 1),
2. *%b.cont. in implant*: percentage of available scaffold outline in contact to bone: [% contact = (bone-scaffold contact length/scaffold outline length)∗100%] in the total implant area (area B in Fig. 1),
3. *%b.cont. in outer zone*: percentage of available scaffold outline in contact to bone: [% contact = (bone-scaffold contact length/scaffold outline length)

Table 2
Implantation scheme

Time (weeks)	Femoral diaphysis			Back muscle		
	Ti	OCP Ti	BCP	Ti	OCP Ti	BCP
6	10	10	10	10	10	10
12	10	10	10	10	10	10

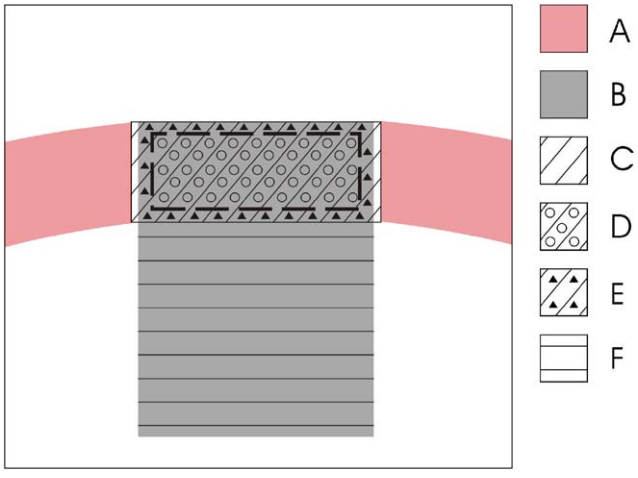

Fig. 1. Zones of histomorphometrical analysis: (A) host cortical bone, (B) total implant area, (C) cortical area, (D) inner zone of the cortical area, (E) outer zone of the cortical area and (F) bone marrow area.

∗100%] in an outer zone of cortical area that is defined as the area of the implant within the cortical area with a thickness of 350 μm measured from the edges of the implant (area E in Fig. 1),

4. *%b.cont. in inner zone*: percentage of available scaffold outline in contact to bone: [% contact = (bone-scaffold contact length/scaffold outline length)∗100%] in the inner zone, that is defined as the area of implant in the total cortical area and excludes the outer zone described in 3) (area D in Fig. 1),
5. *%b.cont. bone marrow*: percentage of available scaffold outline in contact to bone: [% contact = (bone-scaffold contact length/scaffold outline length)∗100%] in the bone marrow area (area F in Fig. 1),
6. *%b. in cortex*: the percentage of bone in available pore area within cortical area (area C in Fig. 1) and
7. *%b. in implant*: the percentage of bone in available pore area in the total implant area (area B in Fig. 1).

We measured de novo bone formation in different areas of the formed defect in order to distinguish new bone formation in the cortical area, where the defect should be healed from the part of the implant that was situated in the bone marrow. Furthermore, we distinguished the outer zone of the cortical area with a thickness of 350 μm, from the inner zone (the rest of the implant) to get more insight into the osteoconductive properties of the materials.

2.7. Statistics

Statistical calculations were done with the SPSS (Chicago, IL) 9.0 software. We found large variances between the individual animals and the data received were not normally distributed. That is why we chose the non-parametric tests to perform the statistical analysis. Friedman rank test, followed by a post hoc test [33] was chosen to make the comparisons between the materials at both time points. Friedman test computes a Friedman two-way analysis of variance on selected variables. This test is a non-parametric extension of the paired *t*-test, where, instead of two measures, each subject has *n* measures ($n > 2$). In other terms, it is a non-parametric analog of repeated measures analyses of variance with one group. The Friedman test is often used for analyzing ranks of three or more objects by multiple judges or like in the case of this study, various materials implanted in all animals. It is used to test the hypothesis that there is no systematic response or pattern across the variables (ratings).

We used the Wilcoxon signed rank test [34] to analyze the difference in bone formation per material between the two time points. The Wilcoxon test compares the rank values of the selected variables, pair by pair, and displays the count of positive and negative differences. For ties, the average rank is assigned. It then computes the sum of ranks associated with positive differences and the sum of ranks associated with negative differences. The test statistic is the lesser of the two sums of ranks.

In both cases, the significance level was set at $p = 0.05$. As can be seen from the descriptions above, the two used statistical tests are both based on ranks, instead of average or median values. However, the results of histomorphometry in this paper are presented in graphs with the average values with standard error of the mean (SEM), in order to make the results more recognizable and comparable with previous studies. And although the asterisks indicating the significant differences are illustrated on these graphs, they are based on the above-mentioned rank tests.

3. Results

3.1. Implant characterization

3.1.1. Uncoated Ti6Al4V

As determined from the material cross-sections, and by the volume/weight method, the porosity of the Ti alloy implants was $79 \pm 5\%$ and the pore size between 400 and 1300 μm. Observations by the ESEM showed that the pores of the implant were well interconnected. Fig. 2a shows the structure of the non-coated porous Ti alloy. Higher magnification photograph (Fig. 2b) shows the rough metal surface, caused by the sintering of the alloy particles.

3.1.2. OCP-coated Ti6Al4V

As observed by the ESEM, in the coated implants, the surface of the Ti alloy was homogeneously covered with a CaP layer. Fig. 3a is a low magnification photograph of the coated Ti6Al4V implant. However, the thickness of the coating was not the same throughout the implant. It varied between 20 μm at the interior of the implant and 60 μm at the implant periphery. Large OCP crystals were oriented perpendicularly to the surface of the metal. Fig. 3b illustrates the crystalline structure of the coating. FTIR spectrum and XRD pattern (Figs. 4a and b, respectively) were typical of the pure, highly crystalline OCP phase. The specific surface area of the coating was $7.2 \pm 0.1\ m^2/g$.

3.1.3. Biphasic calcium phosphate

As observed by the ESEM, BCP implants consisted of a well-interconnected macroporous structure, with a pore size varying between 100 and 800 μm. Histomorphometry on cross-section and determination by the volume/weight method gave an average macroporosity of $54 \pm 4\%$. Higher magnification ESEM analysis showed that macropore walls contained micropores

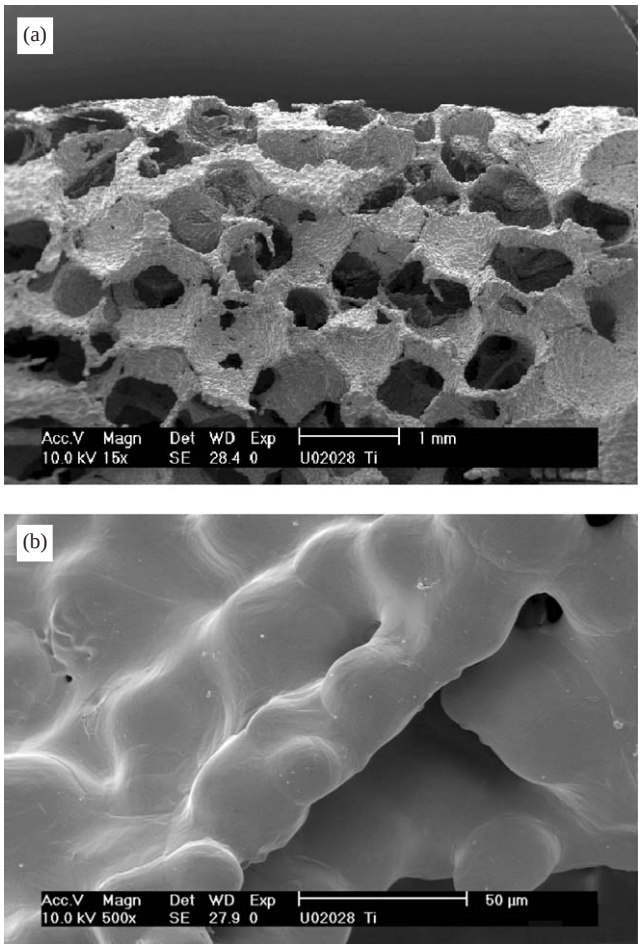

Fig. 2. ESEM photographs of porous Ti6Al4V implant magnification 15× (a) and 500× (b).

(pore size $<10\,\mu m$). Fig. 5a illustrates the macroporous structure of the BCP, while higher magnification photograph (Fig. 5b) shows its micropores. FTIR and XRD analysis of the produced material (Figs. 6a and b, respectively) showed a biphasic chemistry consisting of ± 88 wt% HA and ± 12 wt% β-TCP. The material was highly crystalline. The specific surface area of the ceramic was $1.2 \pm 0.1\,m^2/g$.

3.2. Transcortical implantation

There were no surgical complications and all implants were retrieved. No macroscopic or microscopic signs of infection were found.

3.3. Comparison of the materials

As can be seen from the results shown in Figs. 7a and b of the measurements in the total implant area, both OCP Ti6Al4V and BCP gave a significantly higher amount of bone as compared to the uncoated Ti6Al4V after 6 weeks of implantation, looking at both %b.cont. in implant and %b. in implant. Furthermore, BCP

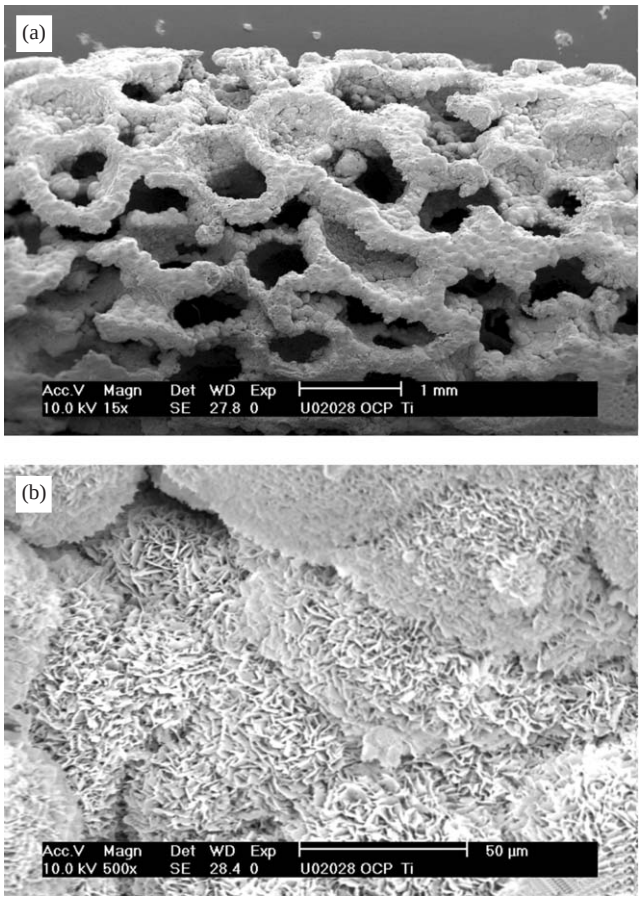

Fig. 3. ESEM photographs of OCP-coated porous Ti6Al4V implant magnification 15× (a) and 500× (b).

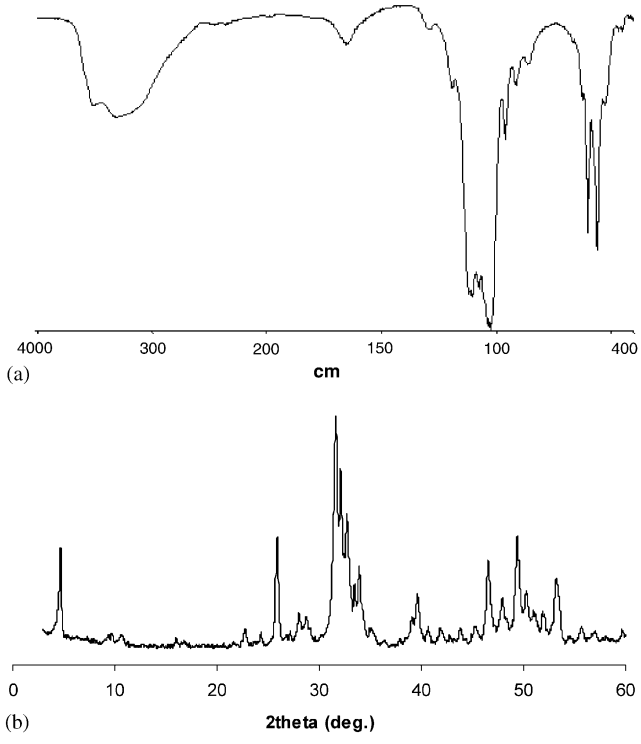

Fig. 4. FTIR spectrum (a) and XRD pattern (b) of the OCP coating.

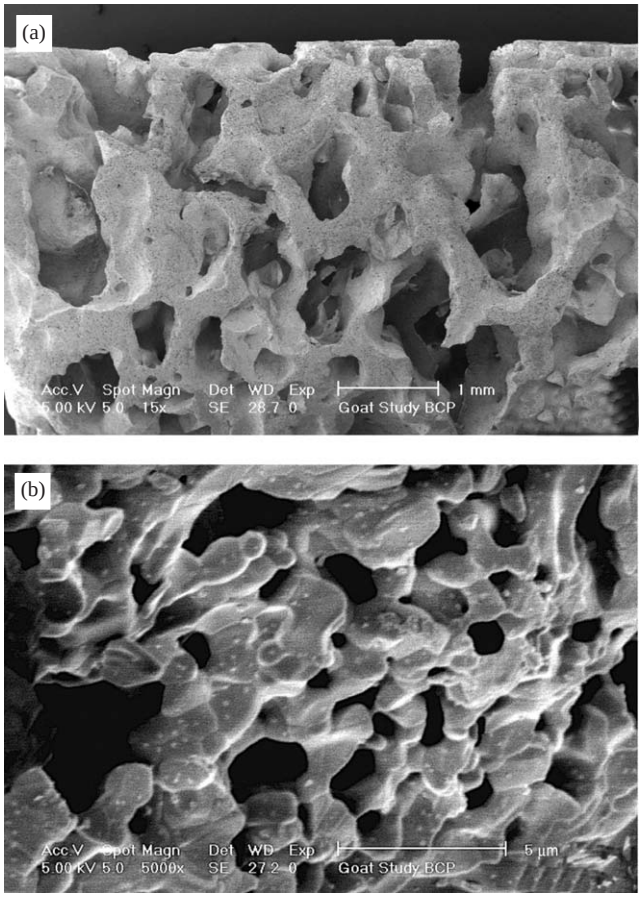

Fig. 5. ESEM photographs of BCP implant magnification 15× (a) and 5000× (b).

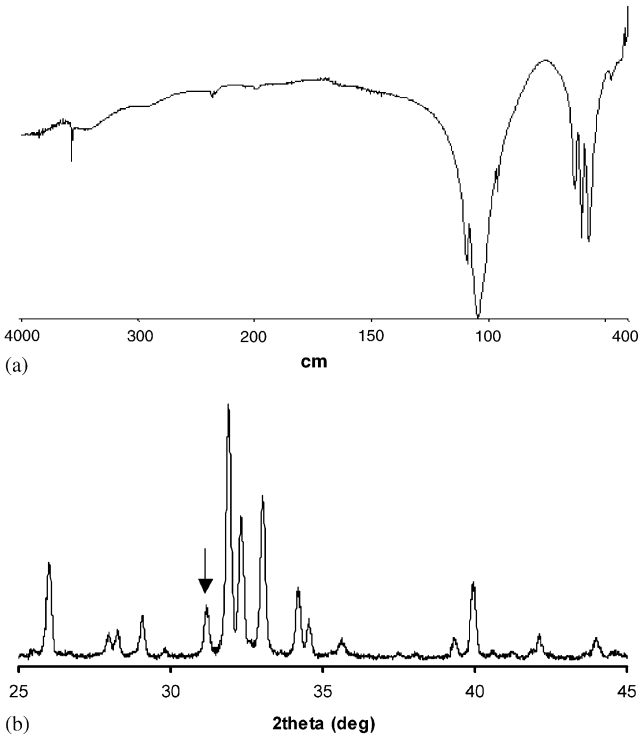

Fig. 6. FTIR spectrum (a) and XRD pattern (b) of BCP ceramic (arrow indicates the main β-TCP peak in BCP).

performed significantly better than OCP Ti6Al4V after 6 weeks. After 12 weeks of implantation, the difference between Ti6Al4V and OCP Ti6Al4V and Ti6Al4V and BCP was still significant, while this was no longer the case for the difference between OCP Ti6Al4V and BCP.

Fig. 8a represents %b.cont. in cortex. After 6 weeks of implantation we can see that the differences between Ti6Al4V and OCP Ti6Al4V and Ti6Al4V and BCP are significant. However, there is no significant difference between OCP Ti6Al4V and BCP that was observed in the graph of the total implant area. Concerning the %b. in the available pore space of the cortical area (Fig. 8b), both OCP Ti6Al4V and BCP are significantly higher than the uncoated Ti6Al4V, and BCP is significantly higher than OCP Ti6Al4V after 6 weeks of implantation. After 12 weeks, however, there are no differences between the three kinds of implants. Figs. 9a, c and e illustrate an example of the bone ingrowth in the cortical area after 6 weeks of implantation in uncoated Ti6Al4V, OCP Ti6Al4V and BCP, respectively. In the case of uncoated Ti6Al4V (Fig. 9a) bone ingrowth starts from the host bone bed toward the implant. In the OCP Ti6Al4V implant (Fig. 9c), new bone had grown deeply into the center of the implant. Similarly, newly formed bone had bridged the formed defect within the BCP implant (Fig. 9e). From the analysis of the histology slides of the implants after 12 weeks of implantation by the light microscope, we observed a lower amount of bone as well as less direct bone contact in the uncoated Ti alloy implants in comparison to both OCP Ti6Al4V and BCP. Fig. 9b is a high magnification of the uncoated Ti alloy after 12 weeks of implantation showing a poor direct contact between metal and bone. Figs. 9d and f, illustrating OCP Ti6Al4V and BCP after 12 weeks of implantation, respectively, show a direct contact between the bone and the material.

When looking at the results illustrated by Fig. 10, we can see significant differences in %b.cont. between Ti6Al4V and OCP Ti6Al4V and between Ti6Al4V and BCP at both time points.

Measurements of %b.cont. in inner and outer zone of the cortical area (not illustrated) showed a significantly higher %b.cont. in the outer zone than in the inner zone after 6 weeks of implantation for each kind of implant. After 12 weeks, however, this difference could only be found for BCP. Differences between the individual materials in both zones were similar to the differences found in the total cortical area (see Fig. 8a), meaning that for both time points in both zones, OCP Ti6Al4V and BCP showed a significantly higher amount of bone contact than the uncoated Ti6Al4V, while there was no difference between BCP and OCP Ti6Al4V.

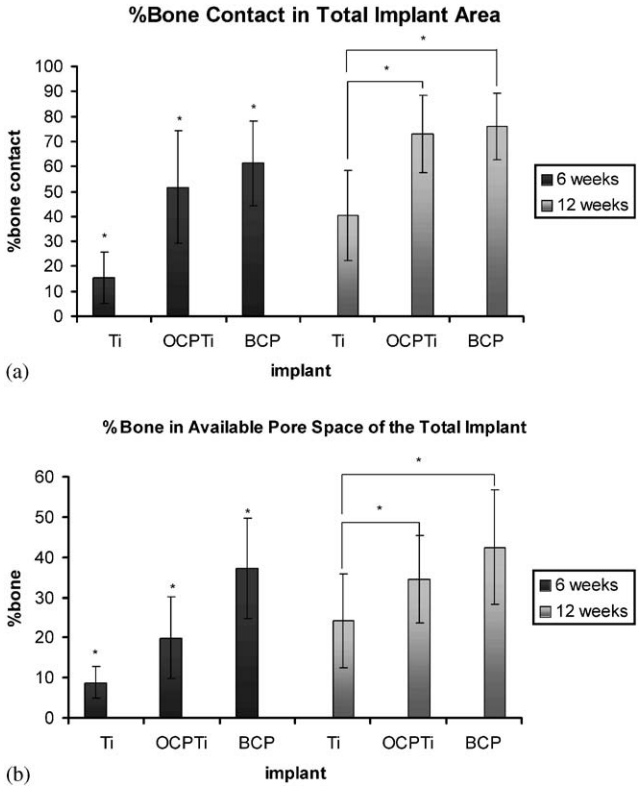

Fig. 7. Histomorphometrical results of the %b.cont. (a) and %b. (b) in total implant area. For both parameters after 6 weeks significant difference ($p = 0.000$ for %b.cont. and $p = 0.001$ for %b.) can be found between OCP Ti6Al4V and Ti6Al4V, between BCP and Ti6Al4V and between BCP and OCP Ti6Al4V; after 12 weeks, significant differences exist between OCP Ti6Al4V and Ti6Al4V and between BCP and Ti6Al4V for both parameters ($p = 0.002$ for %b.cont. and $p = 0.008$ for %b.). According to the Wilcoxon test, significant difference between 6 and 12 weeks was found for the uncoated Ti6Al4V for both %b.cont. ($p = 0.022$) and %b. (0.009) and for OCP Ti6Al4V only for parameter %b. ($p = 0.005$).

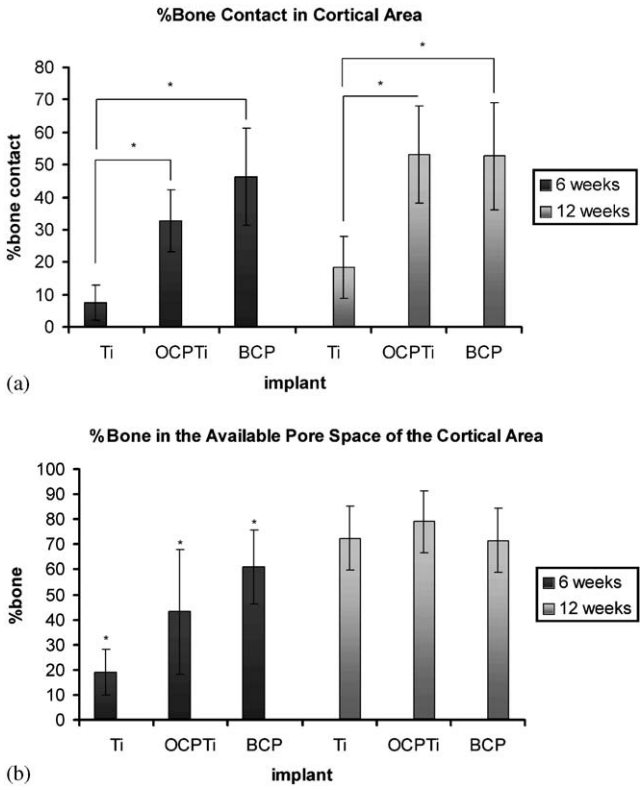

Fig. 8. Histomorphometrical results of the %b.cont. (a) and %b. (b) in cortical area. For parameter %b.cont, after both 6 ($p = 0.000$) and 12 ($p = 0.020$) weeks significant difference can be found between OCP Ti6Al4V and Ti6Al4V and between BCP and Ti6Al4V. For the parameter %b., after 6 weeks ($p = 0.002$) significant difference can be found between OCP Ti6Al4V and Ti6Al4V, between BCP and Ti6Al4V and between BCP and OCP Ti6Al4V. After 12 weeks ($p = 0.273$), no significant differences can be found. Wilcoxon test showed significant difference between 6 and 12 weeks for the uncoated Ti6Al4V for both %b.cont. (0.007) and %b. (0.005). Similarly, for OCP Ti6Al4V there was a significant difference between 6 and 12 weeks in both %b.cont. (0.017) and %b. (0.008).

3.4. Time dependence

Wilcoxon test was used to statistically compare individual materials at the two time points. The test showed significant difference between 6 and 12 weeks of implantation for the uncoated Ti6Al4V in the parameters: %b.cont. in cortex, %b. cortex, %b.cont. in implant, %b. in implant and %b.cont. in inner zone. Significant difference in the OCP Ti6Al4V was found in the parameters: %b.cont. in cortex, %b. in cortex, %b. in implant and %b.cont. in inner zone. No difference between 6 and 12 weeks of implantation in the BCP implants could be found for any of the measured parameters.

3.5. Intramuscular implantation

At retrieval, all implants were surrounded by well-vascularized muscle tissue. Histology showed no evidence for toxicity of the implants nor were the signs of an inflammatory tissue response specifically related to the implants observed.

As observed by light microscopy, uncoated Ti alloy implants did not induce bone in the soft tissue. The implants were, however, extensively filled with fibrous tissue, which is illustrated by Fig. 11a.

Both OCP-coated Ti alloy and BCP (Figs. 11b and c), on the other hand, did show extraskeletal bone formation. Although bone was consistently observed, it occurred in small volumes only. Table 3 gives an overview of the bone incidence in time. In the case of both OCP Ti6Al4V and BCP, more goats showed bone formation after 12 weeks than after 6 weeks. Furthermore, although the bone areas were not measured, the LM analyses of the histological slides suggested an increased amount of formed bone after 12 weeks of implantation when compared to 6 weeks of implantation. The bone was never observed on the implant

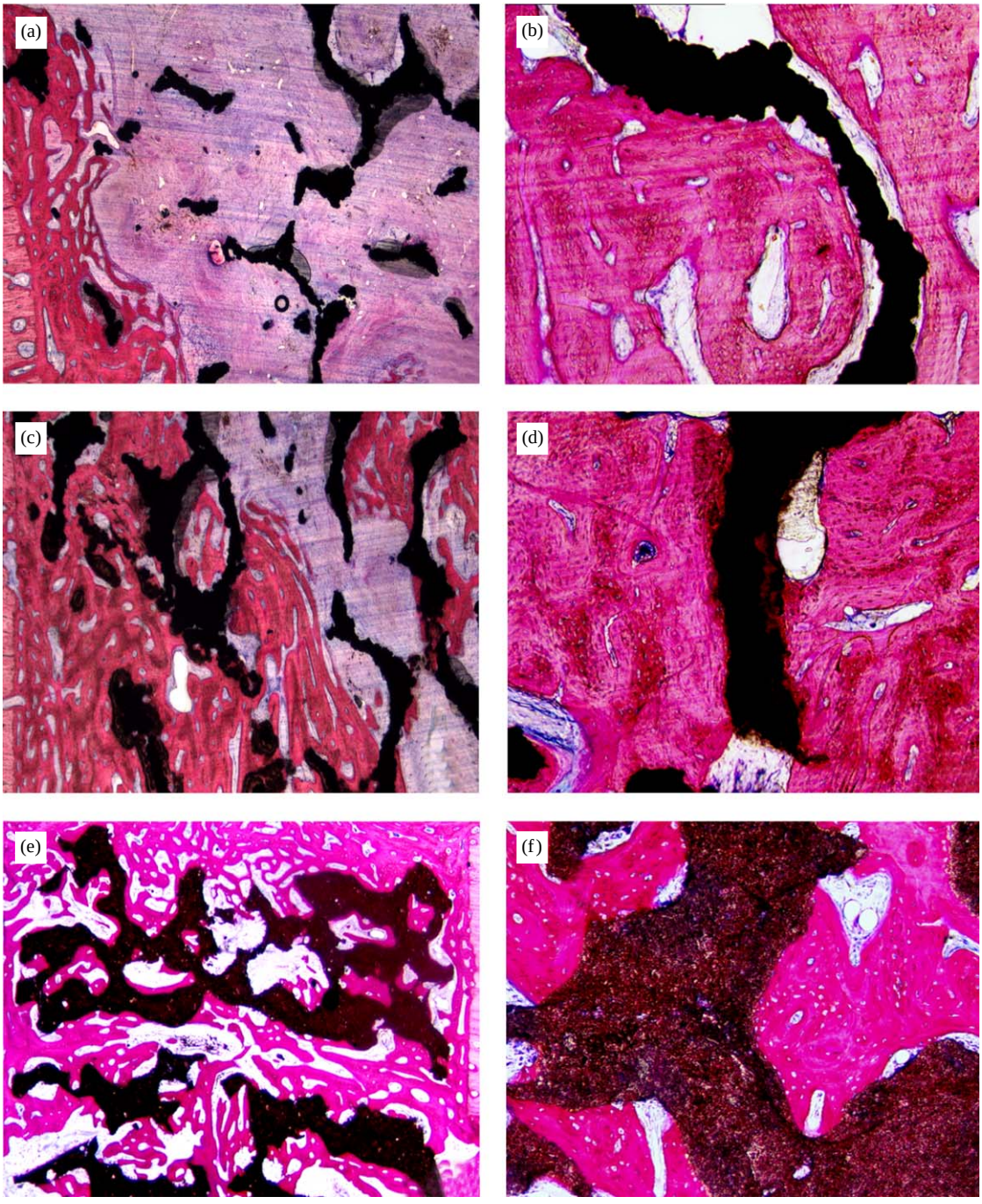

Fig. 9. LM photographs of histological slides of uncoated Ti6Al4V after 6 weeks (magnification 2 ×) (a) and 12 weeks (magnification 10 ×) (b); OCP-coated Ti6Al4V after 6 weeks (magnification 2 ×) (c) and 12 weeks (magnification 10 ×) (d) and BCP after 6 weeks (magnification 2 ×) (e) and 12 weeks (magnification 10 ×) (f) of transcortical implantation. More bone has grown in the OCP Ti6Al4V and BCP (a and c) implants in comparison to the uncoated Ti6Al4V implant (e). Similarly, there is more direct bone contact between the newly formed bone in OCP Ti6Al4V and BCP implants (b and d) in comparison to the uncoated Ti6Al4V implants (f).

periphery, and was always found inside the pores. The formed bone was normal in appearance, aligned with osteoblasts, and with mineralized bone matrix and osteocytes clearly visible. In the case of OCP-coated Ti alloy implants, the coating was often incorporated into the newly formed bone.

Observations of the histological slides of the coated Ti6Al4V implants by LM showed that the OCP coating had extensively dissolved after 6 weeks, and could only occasionally be observed after 12 weeks of implantation, in particular on the periphery of the implant, where the initial coating was the thickest. OCP coating has a

typical crystalline structure that can easily be distinguished from bone on histological slides. The exact dissolution of the coating was, however, not measured. Similar in vivo dissolution behavior of the OCP coating has previously been described [29]. Figs. 12a and b are examples of dissolved OCP coating after 6 and 12 weeks of implantation, respectively. In the areas where the coating was still visible, signs of its resorption by multinucleated cells could be observed, as shown in Fig. 12c. In vitro resorption of OCP coating has previously been shown by Leeuwenbergh et al. [35].

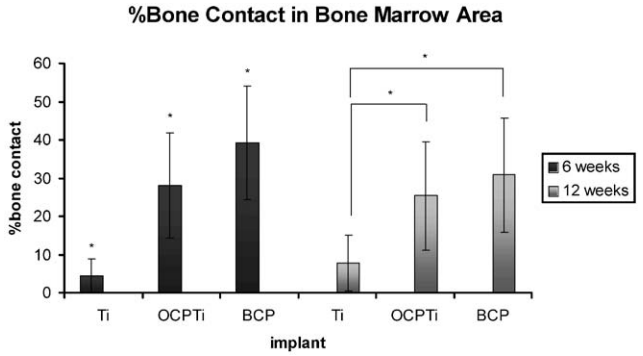

Fig. 10. Histomorphometrical results of the %b.cont. in bone marrow area. After 6 weeks ($p = 0.000$) significant difference can be found between OCP Ti6Al4V and Ti6Al4V, between BCP and Ti6Al4V and between BCP and OCP Ti6Al4V. After 12 weeks ($p = 0.001$), significant differences exist between OCP Ti6Al4V and Ti6Al4V and between BCP and Ti6Al4V. Wilcoxon test did not show significant differences between 6 and 12 weeks for any of the implant groups.

4. Discussion

In this goat study, we investigated the in vivo behavior of a porous Ti6Al4V material, produced by a positive replica method, uncoated and coated with a biomimetic OCP coating, in ectopic and orthotopic locations. We chose BCP ceramic as a reference, because previous animal studies have shown that this material has a large osteoinductive potential [32,36–38] and could possibly be good bone filler in the clinic [39].

Table 3
Bone incidence after intramuscular implantation

Implant	6 weeks	12 weeks
Uncoated Ti6Al4V	0/10	0/10
OCP-coated Ti6Al4V	4/10	6/10
BCP	3/10	6/10

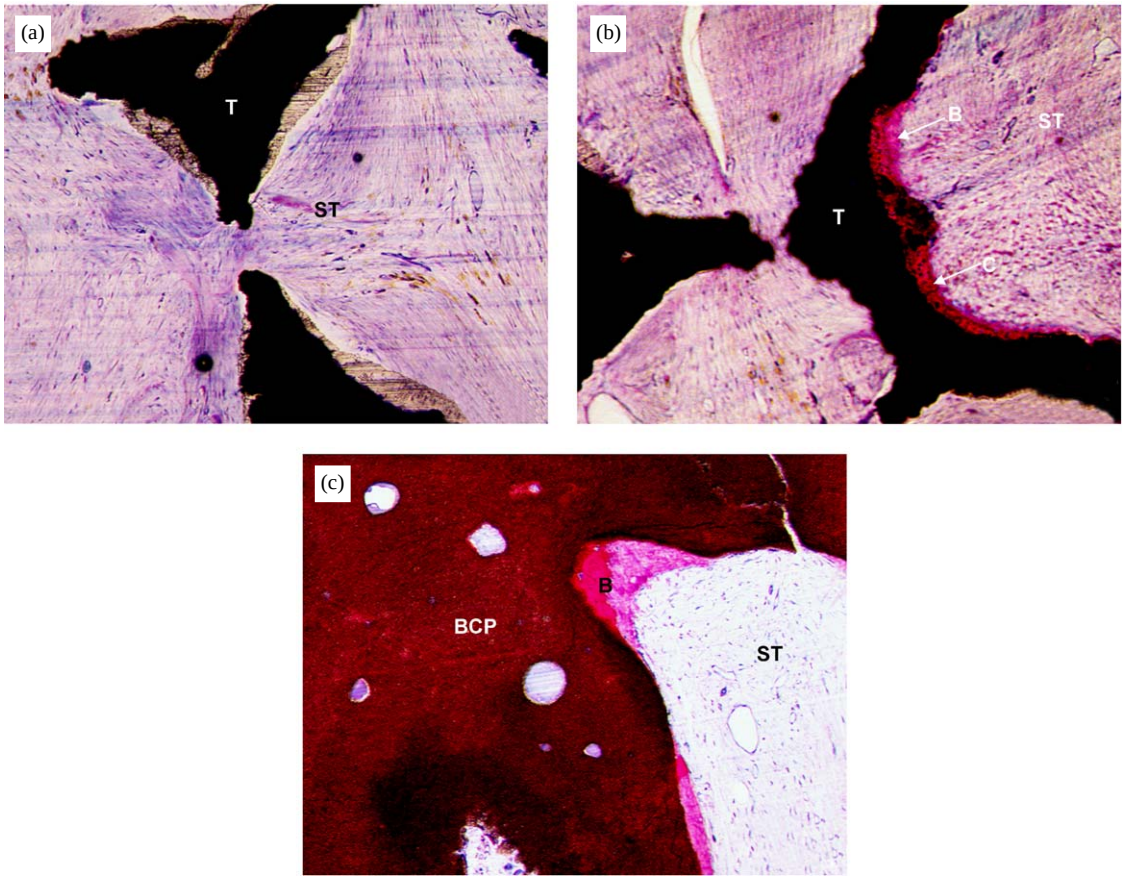

Fig. 11. LM photographs of histological slides magnification 10× of uncoated Ti6Al4V (a), OCP-coated Ti6Al4V (b) and BCP (c) after 12 weeks of intramuscular implantation: T = Ti6Al4V, B = bone, ST = soft tissue, C = OCP coating and BCP = ceramic.

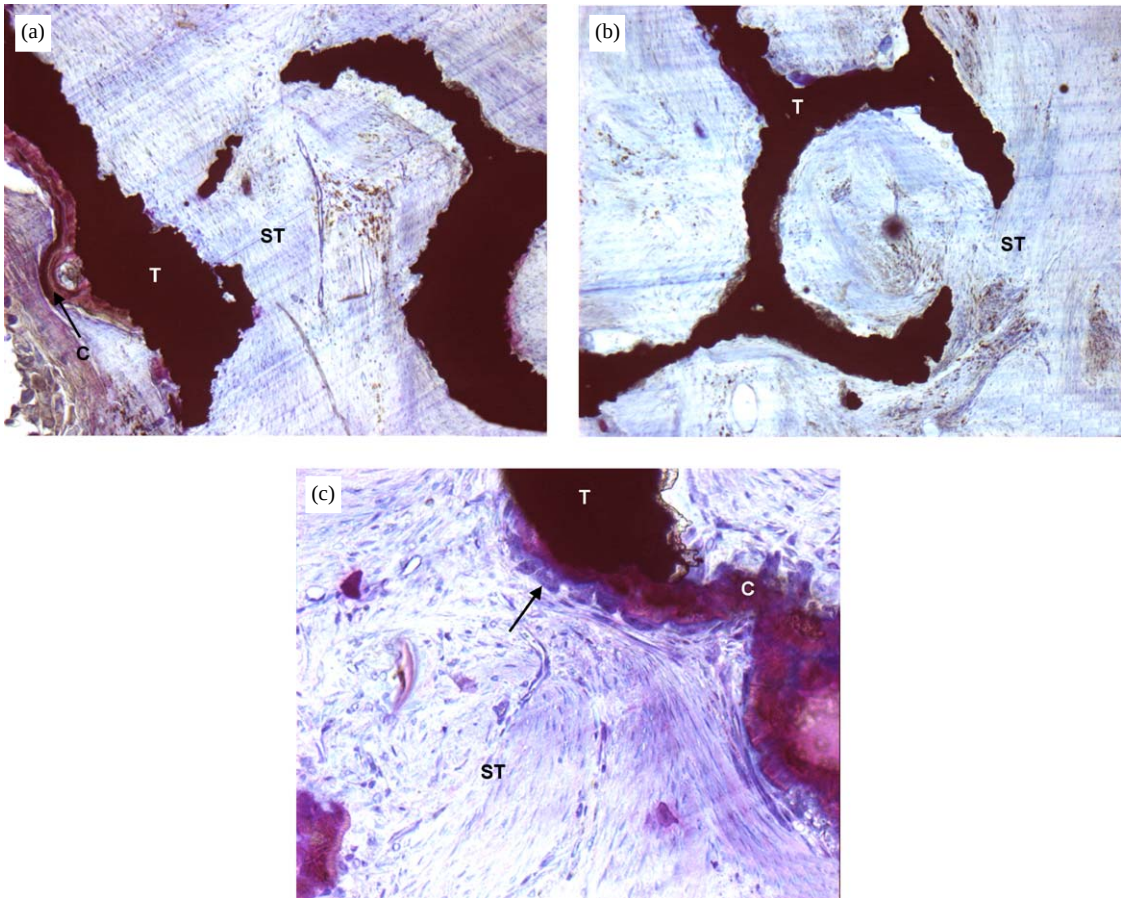

Fig. 12. LM photographs of histological slides magnification 5× of the OCP Ti6Al4V after 6 weeks (a) and 12 weeks (b) of implantation, and magnification 20× after 6 weeks of implantation: T = Ti6Al4V, B = bone, ST = soft tissue, C = OCP coating and BCP = ceramic. In (a) there is still some coating present on the periphery of the implant after 6 weeks of implantation, in (b) after 12 weeks of implantation the coating is further degraded, in (c) multinucleated cells (see arrow) are resorbing the coating left after 6 weeks of implantation.

We introduced a porous structure into all used implants in order to improve mechanical interlocking, and therewith also the bone integration process. However, because of different production techniques, the porosity and the average pore size varied between the metal and the ceramic implants.

As we did not find any signs of toxicity or deviating inflammation related to the implants, we can conclude that our novel material has an acceptable biocompatibility as bone filler. However, the ability of metal itself to guide new bone formation and to form a tight bond with the newly formed bone, i.e. its osteoconductivity [40] is limited. By modification of its surface chemistry and topography, through the application of a CaP coating, we tried to enhance its bioactivity.

Although BCP ceramic, with its high osteoinductive potential and good performance as a bone filler was a good positive control in this study, it is important to note that it had a lower porosity and average pore size than Ti6Al4V and OCP Ti6Al4V. The chemistry of the BCP, that is a mixture of HA and β-TCP, and the biomimetically produced OCP differed as well. Furthermore, due to the sintering process, BCP ceramic macropore walls consisted of micropores, increasing therewith the surface roughness. Such a microporosity was not present in the OCP coating. Nevertheless, OCP coating surface was rough as well, due to the large crystals that were perpendicularly oriented to the metal surface.

The above-mentioned material characteristics: chemical composition, macroporosity, crystallinity and surface roughness are all of great importance for the bone integration process. The release of calcium and phosphate ions is believed to be at the origin of the bioactivity of CaPs [41–43]. This dissolution is followed by the precipitation of a biological CaP layer [44]. In addition, organic compounds are incorporated into this newly formed layer, and cells like osteoprogenitor cells, osteoblasts and osteoclasts colonize the biomaterial [45,46].

Transcortical implantation results of this study confirmed a well-known fact that the application of a CaP layer on a metal surface significantly increases its bioactivity. Biomimetically produced OCP coating applied on our porous Ti6Al4V metal enhances its

osteoconductive properties, while keeping its mechanical strength. Differences in the amount of newly formed bone between the coated and the uncoated Ti alloy implants were significant in the cortical area of the defect as well as in the bone marrow, suggesting a high osteoconductive potential of the OCP coating. We found a significant difference between Ti6Al4V and OCP Ti6Al4V after 12 weeks of implantation in the contact between the newly formed bone and the implant surface, but this difference could not be found in the amount of formed bone in the available pore area. In order to get a full overview of both osteoconductive properties of a material and defect healing process by the material, both histomorphometric methods should be used.

BCP as bulk ceramic caused a faster bone growth, when looking at both bone contact and bone area, in comparison to the OCP as coating on the metal implant. The BET measurements showed that OCP had a specific surface area that was about five times higher than that of BCP. Furthermore, the solubility isotherms of various CaPs show that OCP powder is slightly more soluble than β-TCP powder, and significantly more soluble than HA powder [47]. Both characteristics suggest a higher dissolution rate of OCP in comparison to the BCP that should be followed by a faster CA formation of the material surface and consequently by a faster bone formation. However, as mentioned earlier, the OCP Ti6Al4V implants had a much higher porosity and pore size as compared with BCP. The lower porosity and average pore size of BCP might have been more suitable for bone ingrowth, possibly because of a better balance between a sufficient nutrient and blood supply into the implant, on the one hand, and a protected area that is necessary to reach the super-saturation of Ca^{2+} and PO_4^{3-} ions, in order to initiate the formation of CA layer, on the other hand, in comparison to the OCP-coated Ti6Al4V implant. This is a possible explanation of the observations from this study. However, due to the many differences in material chemistry and morphology between OCP and BCP, further investigations are needed to fully understand their effect on the bone ingrowth.

The difference in the bone amount formed in BCP and OCP Ti6Al4V disappeared after 12 weeks of implantation, which suggests that, on longer term, both CaP materials have the same effect on the bone integration process. This could be explained by the fact that, on longer term, surface of both materials is covered by a bone like CA layer, and that the effect of dissolution behavior of the initial materials became less relevant. In the case of OCP, the coating is fully replaced by the newly formed bone within approximately 12 weeks, and bone continues to grow until the defect is filled. The bulk ceramic, on the other hand, will undergo the same process, but in this case material degradation will continue as well, although very slowly. Comparison of the amount of formed bone between 6 and 12 weeks showed a difference for Ti6Al4V and OCP Ti6Al4V but not for BCP. This once again supports our observation that the bone formation in BCP scaffolds is taking place faster than in the other two materials.

From the results of the intramuscular implantation, we can conclude that uncoated Ti alloy was not osteoinductive in this study, while both OCP Ti6Al4V and BCP did show some extraskeletal bone formation. The amount of formed bone, and the number of animals in which the bone was induced, was similar for the both biomaterials. Although the bone was consistently found, its amount was limited.

It is interesting to note that very large differences were observed between the amount of bone that was induced in individual animals, i.e. one goat was ''more inductive'' than another goat, for all implanted materials. The reason for these differences could be searched in genetic as well as in pathological backgrounds, but as long as the mechanism of osteoinduction itself is not clear, this phenomenon will be hard to explain. Because of such a limited amount of induced bone, any statistical analysis was impossible to perform. The only conclusion is therefore that both BCP and OCP Ti6Al4V have an osteoinductive potential, and that a non-inductive material such as Ti alloy can become inductive by combining it with a CaP coating. The findings from this study would therefore suggest that the presence of CaP is a critical factor in the process of osteoinduction. And although Yuan et al. [48] and Fujibayashi et al. [15] showed the possibility of bone induction by alumina ceramic and chemically treated porous titanium, respectively, most of the biomaterials that were shown to induce bone consist of CaP. Although we know that many different material characteristics (chemistry, composition, macro- and microstructure) may be important for its osteoinductive behavior [32,49–51], the exact mechanism of osteoinduction remains unknown. Concerning this mechanism, we hypothesize: (1) osteoinductive materials exert a direct effect on the growth and differentiation of relevant cells that attach to them, and (2) the surface of osteoinductive materials helps collecting relevant proteins, which in their turn exert an osteoinductive effect on the recruited cells. To test these hypotheses, and to investigate which cells are important in the process of osteoinduction, additional research needs to be performed.

In our study, CaP containing materials are performing better than the bare metal both ectopically and orthotopically, but from our observation, we cannot draw the conclusion that osteoinductivity improves the ingrowth in orthotopic sites, because of the fact that Ti6Al4V is not only non-inductive, but its conductive properties are limited as well. Nevertheless, it has been reported that osteoinductive materials are performing

better orthotopically than the non-inductive materials [52]. This suggests that increased bone ingrowth in OCP Ti6Al4V is not only due to increased osteoconductivity but also due to osteoinductivity of the OCP coating. And although we still neither completely understand the mechanism of osteoinduction nor the effect of osteoinductive properties of the materials when implanted orthotopically, these first results suggest the potential relevance of osteoinductivity for the clinic.

5. Conclusion

In our study, we introduced a porous Ti6Al4V material, produced by a novel technique, with sufficient mechanical properties and biocompatibility. Furthermore, we have shown that the application of OCP coating on the metal implants can improve its performance in bone healing process. BCP ceramic showed better osteoconductive properties than both, uncoated and OCP-coated Ti alloy. Finally, both OCP Ti6Al4V and BCP showed an osteoinductive potential in the muscles of goats.

Acknowledgements

The authors thank Dr. Maarten Terlouw from the Image Analysis Department of the University Utrecht for developing the software used for the histomorphometry and Dr. Paul Westers and Dr. Edwin Martens from the Biostatistics Department for their generous help with statistical analysis.

A part of this study was financially supported by the EU "Intelliscaf" Project (G5RD-CT-2002-00697).

References

[1] Manley MT. Calcium phosphate biomaterials: a review of the literature. In: Geesink RGT, Manley MT, editors. Hydroxyapatite coatings in orthopaedic surgery. New York: Raven Press; 1993. p. 1–19.
[2] Damien CJ, Parsons JR. Bone graft, bone graft substitutes: a review of current technology and applications. J Appl Biomater 1991;2:187–208.
[3] Osborn JF. The biological profile of hydroxyapatite ceramics with respect to the cellular dynamics and human soft tissue and mineralized tissue under loaded and unloaded conditions. In: Barbosa MA, editor. Biomaterials degradation. Amsterdam: Elsevier; 1991. p. 185–225.
[4] Hollinger JO, Brekke J, Gruskin E, Lee D. Role of bone substitute. Clin Orthop 1996;324:55–66.
[5] Daculsi G, Laboux O, Malard O, Weiss P. Current state of the art of biphasic calcium phosphate bioceramics. J Mater Sci: Mater Med 2003;14:195–200.
[6] Agrawal CM. Reconstructing the human body using biomaterials. JOM 1998;50:31–5.
[7] Turner TM, Sumner DR, Urban RM, Rivero DP, Galante JO. A comparative study of porous coatings in a weight-bearing total hip-arthroplasty model. J Bone Jt Surg Am 1986;68(9):1396–409.
[8] Tengvall P, Lundstrom I. Physico-chemical considerations of titanium as biomaterial. Clin Mater 1992;9:115–34.
[9] Hildebrand HF, Hornez JC. Biological response and biocompatibility. In: Helsen JA, Breme HJ, editors. Metals as biomaterials. Chichester: Wiley; 1998. p. 265–90.
[10] Pilliar RM. Porous-surfaced metallic implants for orthopedic applications. J Biomed Mater Res: Appl Biomater 1987;21A(1 Suppl.):1–33.
[11] Pilliar RM. Overview of surface variability of metallic endosseous dental implants: textured and porous-structured designs. Implant Dent 1998;7(4):305–14.
[12] Jaffe WL. Current concepts review: total hip arthroplasty with hydroxyapatite-coated prostheses. J Bone Jt Surg Am 1996;78(12):1918–34.
[13] Bhardwaj T, Pilliar RM, Grynpas MD, Kandel RA. Effect of material geometry on cartilaginous tissue formation in vitro. J Biomed Mater Res 2001;57:190–9.
[14] Wu Bende, Guo Fuhe. A study of preparation of man-made hipbone by using composite porous titanium. Technol Powder Metall 1990;8(4):145–9.
[15] Fujibayashi S, Neo M, Kim HM, Kokubo T, Nakamura T. Osteoinduction of porous bioactive titanium metal. Biomaterials 2004;25(3):443–50.
[16] Jansen JA, von Recum AF, van der Waerden JP, de Groot K. Soft tissue response to different types of fibre-web materials. Biomaterials 1992;13:959–68.
[17] Ferretti C, Ripamonti U. Human segmental mandibular defects treated with naturally derived bone morphogenetic proteins. J Craniofac Surg 2002;13:434–44.
[18] Vohof JW, Takita H, Kuboki Y, Spauwen PH, Jansen JA. Histological characterization of the early stages of bone morphogenetic protein-induced osteogenisis. J Biomed Mater Res 2002;61(3):440–9.
[19] van den Dolder J, Farber E, Spauwen PHM, Jansen JA. Bone tissue reconstruction using titanium fiber mesh combined with rat bone marrow stromal cells. Biomaterials 2003;24:1745–50.
[20] Sikavitsas VI, van den Dolder J, Bancroft JN, Jansen JA, Mikos AG. Influence of the in vitro culture period on the in vivo performance of cell/titanium bone tissue engineered constructs using a rat cranial critical size defect model. J Biomed Mater Res 2003;67A(3):944–51.
[21] Zardiackas LD, Douglas EP, Lance DD, Darrell WM, Nunnery LA, Poggie R. Structure, metallurgy, and mechanical properties of a porous tantalum foam. J Biomed Mater Res (Appl Biomater) 2001;58:180–97.
[22] Bobyn JD, Stackpool GJ, Hacking SA, Tanzer M, Kryger JJ. Characteristics of bone ingrowth and interface mechanics of a new porous tantalum biomaterial. J Bone Jt Surg Br 1999;81-B(5):907–14.
[23] Sidhu KS, Prochnow TD, Schmitt P, Fischgrund J, Weisbrode S, Herkowitz HN. Anterior cervical interbody fusion with rhBMP-2 and tantalum in a goat model. Spine J 2001;1:331–40.
[24] Li JP, Li SH, de Groot K, Layrolle P. Preparation and characterization of porous titanium. Key Eng Mater 2002;218–220:51–4.
[25] Havelin LI, Engesaeter LB, Espehaug B, Furnes O, Lie SA, Vollset SE. The Norwegian arthroplasty register, 11 years and 73,000 arthroplasties. Acta Orthop Scand 2000;71(4):337–53.
[26] Kokubo T, Kushitani H, Sakka S, Kitsugi T, Yamamuro T. Solutions able to reproduce in vivo surface-structure changes in bioactive glass-ceramics A-W3. J Biomed Mater Res 1990;24:721–34.

[27] Barrère F, Layrolle P, van Blitterswijk CA, de Groot K. Biomimetic calcium phosphate coatings on Ti6Al4V: growth study of OCP. J Mater Sci Mater Med 2001;12:529–34.
[28] Habibovic P, Barrère F, van Blitterswijk CA, de Groot K, Layrolle P. Biomimetic hydroxyapatite coating on metal implants. J Am Ceram Soc 2002;85(3):517–22.
[29] Barrère F, van der Valk CM, Dalmeijer RAJ, Meijer G, van Blitterswijk CA, de Groot K, Layrolle P. Osteogenicity of octacalcium phosphate coatings applied on porous metallic implants. J Biomed Mater Res 2003;66A(4):779–88.
[30] Yuan H, de Bruijn JD, Dalmeijer R, Layrolle P, van Blitterswijk CA, Xingdong Z, de Groot K. Bone induction through physicochemistry. PhD thesis, Osteoinduction by Calcium Phosphates, Leiden University, The Netherlands, 2001. p. 123–31.
[31] de Bruijn JD, Yuan H, Dekker R, Layrolle P, de Groot K, van Blitterswijk CA. Osteoinductive biomimetic calcium-phosphate coatings and their potential use as tissue-engineering scaffolds. In: Davies JE, editor. Bone engineering. Toronto: University of Toronto Press; 2000. p. 421–31.
[32] Yuan H, van den Doel M, Li SH, van Blitterswijk CA, de Groot K, de Bruijn JD. A Comparison of the osteoinductive potential of two calcium phosphate ceramics implanted intramuscularly in goats. J Mater Sci Mater Med 2002;13:1271–5.
[33] Hollander M, Wolfe DA. Nonparametric statistical inference. New York: Wiley; 1973. p. 139–46.
[34] Mendenhall W. Nonparametric statistics: introduction to probability and statistics, 3rd ed. Belmont: Duxbury Press; 1971. p. 379–82.
[35] Leeuwenbergh S, Layrolle P, Barrère F, de Bruijn JD, Schoonman J, van Blitterswijk CA, de Groot K. Osteoclastic resorption of biomimetic calcium phosphate coatings in vitro. J Biomed Mater Res 2001;56:208–15.
[36] Gosain AK, Song L, Riordan P, Amarante MT, Nagy PG, Wilson CR, Toth JM, Ricci JL. A 1-year study of osteoinduction in hydroxyapatite-derived biomaterials in an adult sheep model: Part I. Plast Reconstr Surg 2002;109:619–30.
[37] Yang Z, Yuan H, Tong W, Zou P, Chen W, Zhang X. Osteogenesis in extraskeletally implanted porous calcium phosphate ceramics: variability among different animals. Biomaterials 1996;17:2131–7.
[38] Yang Z, Yuan H, Zou P, Tong W, Qu S, Zhang X. Osteogenic response to extraskeletally implanted synthetic porous calcium phosphate ceramics: an early stage histomorphological study in dogs. J Mater Sci Mater Med 1997;8:697–701.
[39] Cavagna R, Daculsi G, Bouler JM. Macroporous calcium phosphate ceramic: a prospective study of 106 cases in lumbar spinal fusion. J Long Term Eff Med Implants 1999;9(4):403–12.
[40] Hench LL, Wilson J. Surface-active biomaterials. Science 1984;226(4675):630–6.
[41] Geesink RG, de Groot K, Klein CP. Bonding of bone to apatite-coated implants. J Bone Jt Surg Br 1988;70B:17–22.
[42] Hanawa T, Kamira Y, Yamamoto S, Kohgo T, Amemyia A, Ukai H, Murakami K, Asaoka K. Early bone formation around calcium-ion-implanted titanium inserted into rat tibia. J Biomed Mater Res 1997;36:131–6.
[43] Kay JF, Cook SD. Biological profile of calcium phosphate coatings. In: Geesink RGT, Manley MT, editors. Hydroxyapatite coatings in orthopaedic surgery. New York: Raven Press; 1993. p. 89–106.
[44] Le Huec JC, Clement D, Brouillaud B, Barthe N, Dupuy B, Foliguet B, Basse-Cathalinat B. Evolution of the local calcium content around irradiated b-tricalcium phosphate ceramic implant: in vivo study in the rabbit. Biomaterials 1998;19:733–8.
[45] Ducheyne P, Bianco P, Radin S, Schepers E. Bioactive materials: mechanism and bioengineering considerations. In: Ducheyne P, Kokubo T, van Blitterswijk CA, editors. Bone-bonding materials. Leiderdorp: Reed Healthcare Communications; 1993. p. 1–12.
[46] LeGeros RZ, Orly I, Gregoire M, Daculsi G. Substrate surface dissolution and interfacial biological mineralization. In: Davies JE, editor. The bone-biomaterial interface. Toronto: University of Toronto Press; 1991. p. 76–87.
[47] Elliot JC. Studies in inorganic chemistry: structure and chemistry of the apatites and other calcium orthophosphates. Amsterdam: Elsevier; 1994. p. 4.
[48] Yuan H, de Bruijn JD, Zhang X, van Blitterswijk CA, de Groot K. Osteoinduction by porous alumina ceramic. Abstract Book of 16th European Conference on Biomaterials, London, 2001. p. 209.
[49] Magan A, Ripamonti U. Geometry of porous hydroxyapatite implants influences osteogenesis in baboons (*Papio ursinus*). J Craniofac Surg 1996;7:71–8.
[50] Yuan H, de Bruijn JD, Li Y, Feng Z, Yang K, de Groot K, Zhang X. Bone formation induced by calcium phosphate ceramics in soft tissue of dogs: a comparative study between α-TCP and β-TCP. J Mater Sci Mater Med 2001;12:7–13.
[51] Yuan H, Kurashina K, de Bruijn JD, Li Y, de Groot K, Zhang X. A preliminary study on osteoinduction of two kinds of calcium phosphate ceramics. Biomaterials 2000;20:1283–90.
[52] Yuan H, de Bruijn JD, van Blitterswijk CA, de Groot K. Osteoinductive biomaterials and bone repairs. Abstract Book of 17th European Conference on Biomaterials, Barcelona 2002, p. 156.